Journal of Marine Research, 56, 489–517, 1998

The tidal and subtidal variations in the transverse salinity and current distributions across a coastal plain estuary

by Kuo-Chuin Wong[1] and Joy E. Moses-Hall[1]

ABSTRACT

The transverse structure in the current and salinity distributions across the mouth of Delaware Bay are examined over the tidal and subtidal time scales. Results show that the across-estuary variation in bathymetry, in the form of a channel-shoal configuration, has a very significant impact on the characteristics of transverse variability. The mean current over the channel is characterized by a strong outflow of low salinity water in the upper layer and a strong inflow of high salinity water in the lower layer, consistent with the density-induced gravitational circulation. The mean flow pattern in the shallow waters over the shoals is marked by transverse rather than vertical variation. The subtidal current and salinity fluctuations are primarily driven by the effect of local atmospheric forcing. The subtidal current fluctuations in the upper layer of the channel are frictionally coupled to the local wind, resulting in downwind currents. The subtidal current fluctuations in the lower layer of the channel, however, flow in the direction of local setup and against the wind. With a wind blowing down the estuary, the wind-induced current tends to reinforce the two-layer structure of the gravitational circulation and substantially enhance the vertical shear and surface to bottom salinity difference. The reverse occurs with a wind in the up-bay direction. The subtidal currents in the shallow areas to the right of the channel exhibit largely depth-independent response to the effect of local wind, with downwind currents at both the surface and the bottom. At tidal frequencies the currents show only a modest variation across the bay mouth. Tidal currents are highly deterministic, but the characteristics of the tidal variability in salinity exhibit significant changes over long time scales. These long-term changes in the intratidal salinity variability are caused by the nonlinear interactions between the tidal and subtidal motions. The residual salt flux through the bay mouth shows significant subtidal fluctuations. The leading factor responsible for producing such subtidal fluctuations is the advection of salt by the wind-induced subtidal currents, but the effect of tidal pumping also contributes significantly to the overall residual salt flux into the estuary.

1. Introduction

Estuarine processes are three-dimensional in nature. Even though the earlier studies tended to focus primarily on the vertical and axial variabilities in estuaries (e.g. Pritchard, 1952, 1956), there is ample evidence from existing literature that significant transverse variability associated with the baroclinic gravitational circulation may exist in many coastal plain estuaries.

1. College of Marine Studies, University of Delaware, Newark, Delaware, 19716, U.S.A.

Fischer (1972) was among the first to suggest the importance of the transverse structure in the density-induced circulation in estuaries. Dyer (1974) showed that the salt balance in two partially mixed estuaries (The Mersey and South Hampton Water) was significantly affected by the transverse variation in the circulation structure. Schroeder (1978) examined the riverine influence on Mobile Bay and found significant transverse variation in the near bottom salinity of up to 10 psu, with saltier water residing in the central portion of the bay while fresher water was found along the shores. Murray and Siripong (1978) examined the tidally averaged salinity distribution across Rio Guayas, a shallow estuary in Ecuador, and found significant lateral variation in the salinity structure which indicates the presence of relatively saline water in the middle of the cross-section and fresher water along the shores. Kjerfve (1978) showed that the distribution of residual circulation may be closely associated with the bottom bathymetry. Based on current measurements from 10 stations across North Inlet, South Carolina, Kjerfve and Proehl (1979) found significant transverse variation in the structure of the tidally averaged current there. Kjerfve (1986) later found that there is a pronounced transverse circulation contribution to the mean advective salt flux at North Inlet.

The transverse structure of the long-term residual motion has received renewed attention in the past few years. This includes the studies conducted by Wong (1994) and Wong and Münchow (1995) in the lower Delaware Bay and by Valle-Levinson *et al.* (1994) and Valle-Levinson and Lwiza (1995, 1997) in the lower Chesapeake Bay. In addition to the observational studies, Friedrichs and Hamrick (1996) and Valle-Levinson and O'Donnell (1996) have conducted analytical and numerical studies to relate the structure of the density-induced residual circulation to the transverse variation in bathmetry commonly found in coastal plain estuaries.

It has been known for some time that the effect of wind may produce significant subtidal variability in estuaries. The modeling studies conducted by Csanady (1973), Hunter and Hearn (1987) and Signell *et al.* (1990) on wind-induced barotropic motion in elongated lakes and coastal embayments indicate that the wind-driven circulation in estuaries with channel-shoal configurations may exhibit significant transverse and vertical variations.

At higher frequencies the estuaries are forced by the astronomical tides from the adjacent continental shelf. Huzzey (1988) and Huzzey and Brubaker (1988) showed that the differential advection between the faster currents over the channel and the slower currents over the shoals produces significant variation in the salinity distribution across the York River estuary. During the flood tide, the differential advection produces higher salinity over the channel and lower salinity over the shoals. The reverse occurs during the ebb tide.

In light of these developments, the present study seeks to establish that the presence of significant transverse variability is an integral part of the response of an estuary to a variety of forcing mechanisms over a broad spectrum of frequencies. Through a systematic examination of a set of current meter data, this study examines the nature and characteris-

tics of the long-term mean distribution as well as the subtidal and tidal fluctuations in the transverse structure of salinity and current in a major coastal plain estuary. For the sake of brevity, the present study focuses on the transverse and vertical variations in the longitudinal component of the current. The characteristics of the transverse circulation will be addressed in a separate paper. Through linear interaction, the transverse variability at any instant in time may deviate significantly from the mean distribution based on a superposition of the various mechanisms. However, there is also evidence that the transverse salinity structure may be affected by the nonlinear interactions between mechanisms operating at different frequencies. This effect is especially evident on the long-term changes in the intratidal salinity variability across the estuary. Furthermore, the contributions of the tidal and subtidal variabilities to the residual advective salt flux are examined.

2. Study area and data sources

Delaware Bay (Fig. 1) is a major coastal plain estuary on the east coast of the United States. It communicates with the Atlantic Ocean through a mouth of 18 km width between Cape Henlopen, Delaware and Cape May, New Jersey. Almost all of the freshwater enters the bay in its narrow reaches north of the C&D Canal. The bathymetry near the bay mouth is quite complicated, with a deep channel running near Cape Henlopen. The part of the bay mouth near Cape May is marked by the presence of extensive shoals.

Salinity and current time series at the mouth of Delaware Bay are available from a survey conducted by the National Ocean Service (NOS) during April 1984. NOS deployed a total of seven current meters on four separate moorings (Fig. 2), but a malfunction of the near-bottom current meter at mooring 2 produced only current measurements but no salinity data at meter 2b. Mooring 1 is located over the deep channel near Cape Henlopen. Mooring 2 is located in the central portion of the bay and moorings 3 and 4 are located in the shallow waters near Cape May. The current meters provide time series data at 10 minute intervals. Details about the NOS survey have been reported by Klavens *et al.* (1986). In addition to the current and salinity data, wind measurements recorded at a NOAA environmental buoy (EB09) off the mouth of the bay are obtained from the National Climatic Data Center. The Delaware River discharge recorded at Trenton, New Jersey is also obtained from the U.S. Geological Survey. Figure 3 shows the observed current and salinity time series at all the current meter locations. For the sake of brevity, only the current components perpendicular to the bay mouth transect, with a positive current representing water flowing into the bay are presented here. All the time series data exhibit a combination of mean values, subtidal fluctuations, and high frequency tidal oscillations. To allow a more in-depth analysis of the transverse salinity variability at different time scales, all the time series are passed through a Lanczos filter (Bloomfield, 1976) with a cutoff period of 36 hours so that the high frequency tidal variability can be separated from the low frequency signals.

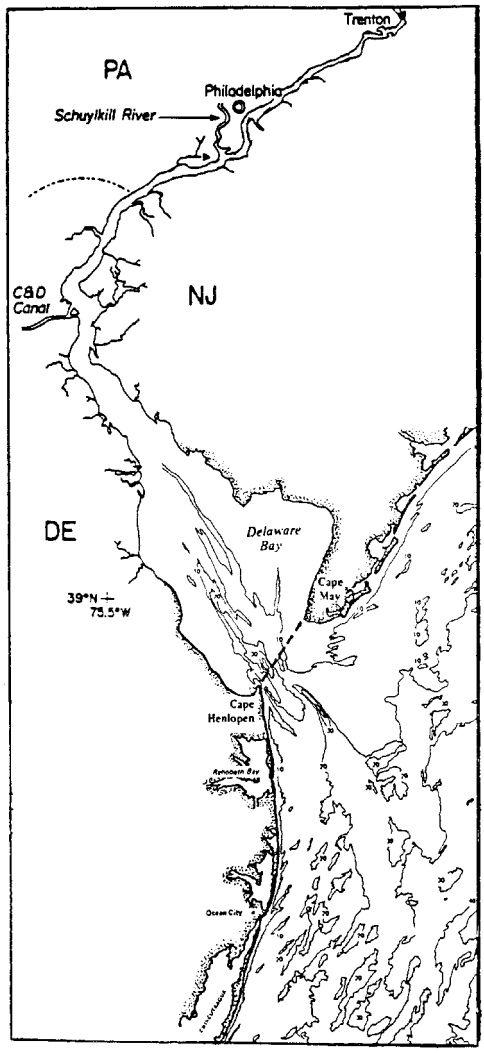

Figure 1. Location map of Delaware Bay. Bathymetry is in meters. The current meter mooring transect is marked by the dashed line.

3. The mean current and salinity distribution

The right panel of Figure 4 shows the mean salinity distribution across the bay mouth. The view is upbay, with the Delaware shore (Cape Henlopen) to the left. Not surprisingly, the water with the highest salinity (28.4 psu) is found in the lower layer of the deep channel near the Delaware shore. The water with the lowest salinity (26.4 psu) is found in the upper layer of the deep channel. Above a depth of about 12 m, the salinity increases as one travels away from the Delaware shore until a local maximum (28.1 psu) is reached in the central portion of the bay. It should be noted that the circular contour lines of 27.8 and 28.0 psu are

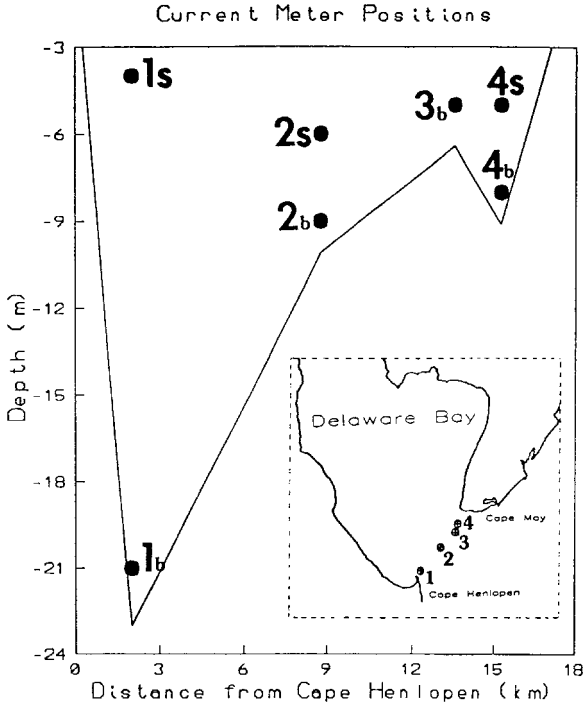

Figure 2. The positions of current meters across the bay mouth transect. The view is up-bay, with the Delaware shore to the left. The subscript "*s*" designates near-surface current meter and the subscript "*b*" designates near-bottom current meter. The insert shows a plan view of the positions of the four moorings.

an artifact of the SURFER interpolation routine. From that point the salinity decreases to about 27.3 psu near the New Jersey shore. The mean salinity distribution thus shows the presence of two branches of low salinity water in the shallow waters along the shores separated by high salinity water in the central part of the bay. The transverse variation in salinity is almost as large as the surface to bottom salinity difference over the deep channel. The branch of low salinity water along the Delaware shore is far more prominent than its counterpart along the New Jersey shore. Both of these features have been qualitatively observed in previously conducted shipboard measurements made over one or two tidal cycles (Wong, 1994). The mean distribution presented here confirms the robustness of the transverse salinity structure.

It is instructive to examine whether there is a close correlation between the mean salinity and current distributions. The left panel of Figure 4 shows the mean flow structure across the bay mouth. Over the deep channel the mean current is marked by a strong outflow (-16 cm/s) in the upper layer and a strong inflow (12 cm/s) at depth. It appears that the mean flow over the channel is consistent with the density-induced gravitational circulation, with a brackish outflow in the upper layer and a more saline inflow in the lower layer. In the

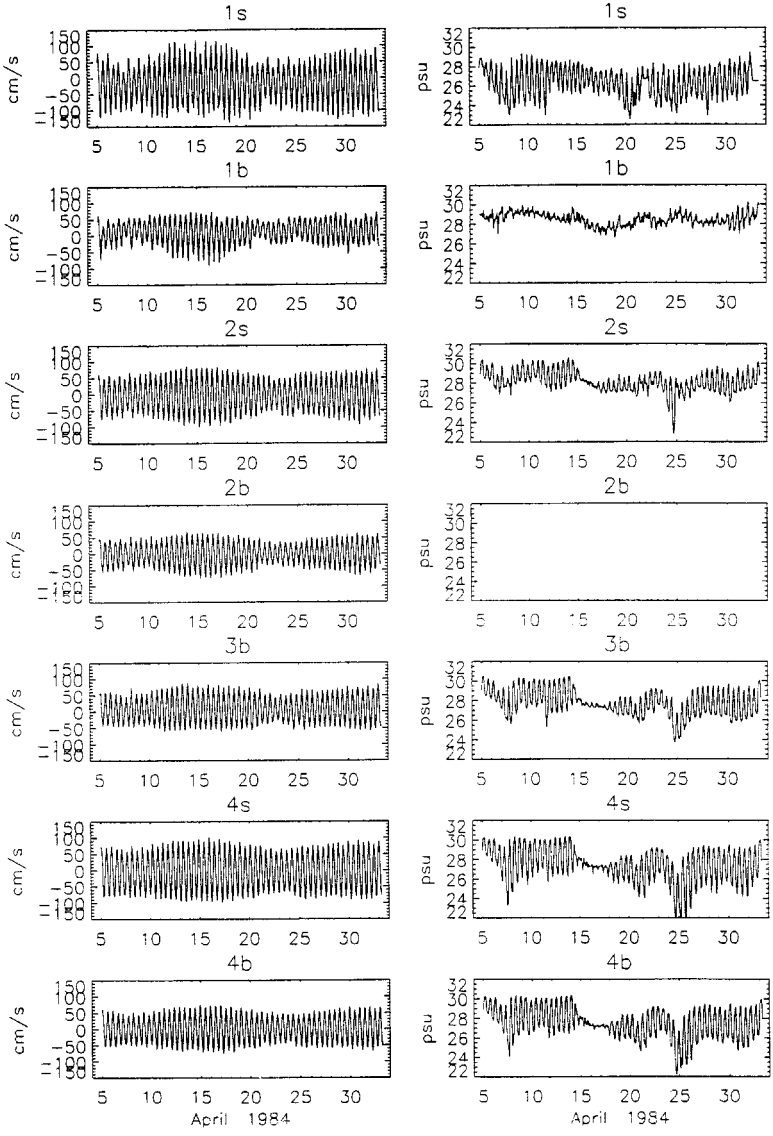

Figure 3. The longitudinal component of currents and salinity at mooring sites 1s, 1b, 2s, 2b, 3b, 4s, and 4b.

shallow region to the right of the channel the flow structure is marked primarily by transverse variation rather than vertical variation. There are alternating bands of inflow and outflow as one travels toward the New Jersey shore, but a reversal of mean flow with depth is not evident in these areas. There is a weak outflow near the New Jersey shore, consistent with the presence of a second branch of low salinity water there. Figure 5 shows a plot of

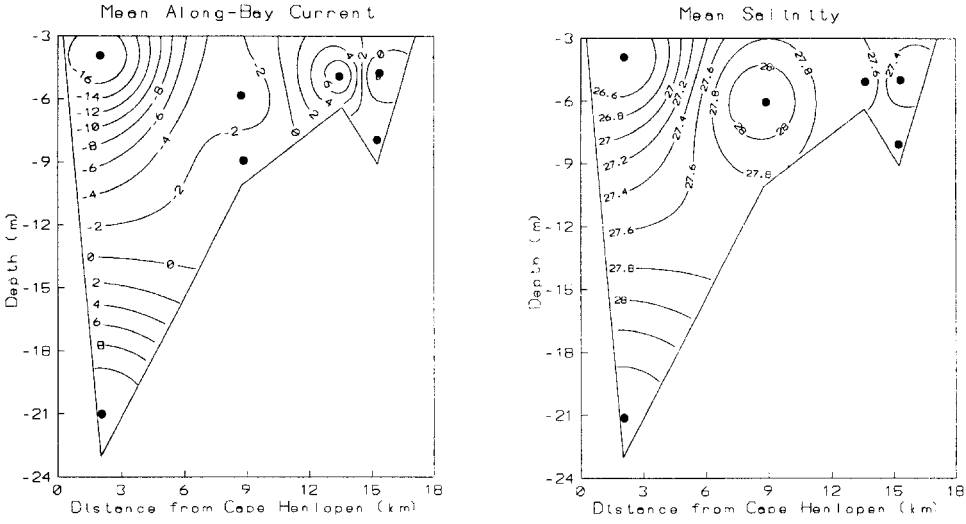

Figure 4. Contours of the mean longitudinal current (left panel) and salinity (right panel) distribution across the bay mouth.

mean flow versus salinity from the 6 mooring sites, with the straight line representing the linear regression between the two. The correlation coefficient between the mean flow and salinity is 0.84, suggesting that outflow is closely associated with low salinity water and vice versa.

4. The subtidal variability

Figure 6 shows the subtidal fluctuations in current (solid line) and salinity (dashed line) at the six sites where both types of measurements are available. The surface and bottom currents at both moorings 1 and 4 are highly correlated. However, currents at mooring 1 (1s and 1b) are negatively correlated with a correlation coefficient of -0.82, indicating that currents in the upper and lower layers are fluctuating in opposite directions to each other. On the other hand, the currents at mooring 4 (4s and 4b) are positively correlated with a correlation coefficient of 0.83, suggesting in-phase fluctuations there. Furthermore, the surface current at mooring 1 over the channel (1s) and that at mooring 4 in the shallow waters off Cape May (4s) are significantly correlated with a correlation coefficient of 0.68, suggesting in-phase fluctuations at the surface. It is important to note, however, that the magnitude of the currents are much stronger over the channel than over the shallow areas off the New Jersey shore.

Spectral analysis reveals that the variance of the subtidal current is concentrated at time scales of 2–5 days. A variety of mechanisms may be responsible for producing the subtidal current fluctuations. These include tidal rectification, river-induced variability, and the combined effect of local and remote atmospheric forcing. Tidal rectification may produce low frequency fluctuations in currents, but its effect is primarily felt at the fortnightly or

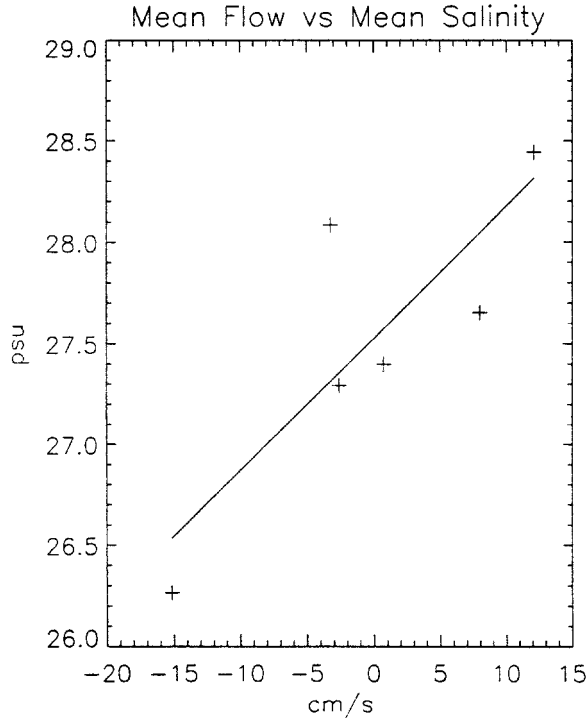

Figure 5. A plot of mean flow versus mean salinity. The straight line represents a linear regression of the data points. The correlation coefficient is 0.84.

monthly periods, not the 2–5 day time scales involved here. River discharge may induce barotropic and baroclinic responses at subtidal frequencies. However, the Delaware River discharge data (Fig. 6) suggest that the freshwater discharge events are too infrequent to produce the 2–5 day variability seen in the subtidal currents.

Remote atmospheric effect can produce subtidal variability within the bay through the set up/set down of subtidal sea level along the open coast. The current is expected to flow into the bay with a coastal set up and vice versa. This effect can be assessed by comparing the sectionally averaged current ($\langle u \rangle$) with the barotropic exchange computed from the continuity requirement. The sectionally averaged barotropic current (dashed line, Fig. 7) is computed as $\langle u \rangle = \Sigma_{j=1}^{7} a_j u_j$ where u_j indicates the observed longitudinal current at the j-th location and a_j is the normalized weight at the j-th location. Since the seven current meters are unevenly distributed across the bay mouth, a different weight is assigned to each current meter so as to more accurately reflect the fractional area it represents over the entire cross-sectional area of the bay mouth. The barotropic current (solid line, Fig. 7) is computed as $\langle u_\eta \rangle = 1/A_m[A_s\ (\partial\eta/\partial t)]$, where A_s is the surface area of the bay, A_m is the cross-sectional area of the bay mouth, and η is the observed surface elevation at Cape Henlopen. For Delaware Bay, $A_s = 2.0 \times 10^9$ m^2 and $A_m = 2.6 \times 10^5$ m^2 (Garvine, 1991).

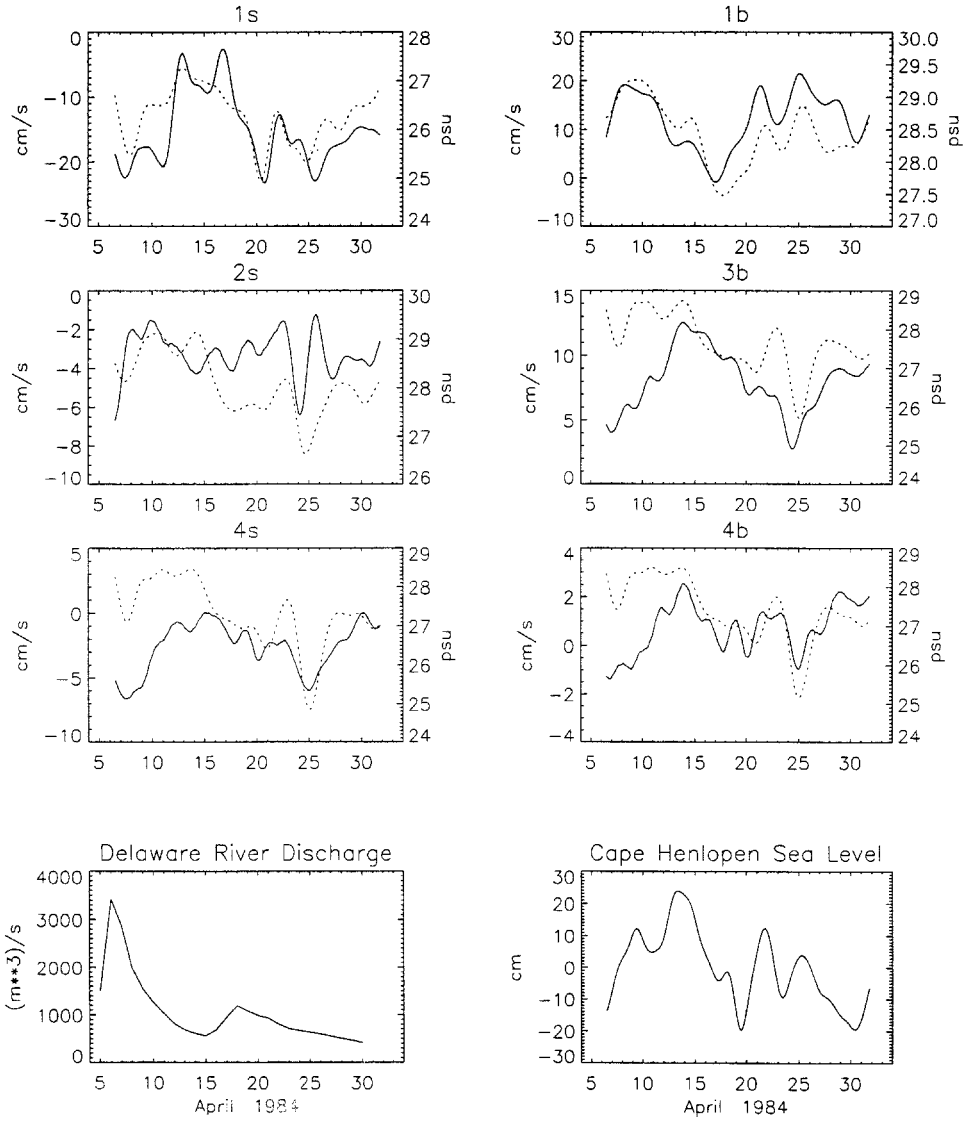

Figure 6. The longitudinal component of the subtidal current (solid line) and salinity (dashed line) at moorings 1s, 1b, 2s, 3b, 4s, and 4b. Plots of the daily Delaware River discharge and the subtidal sea level fluctuations at Cape Henlopen are also shown.

$\langle u_\eta \rangle$ represents the lowest order response of the bay to remote (coastal sea level) forcing, with inflow corresponding to a rise in sea level and vice versa. It would represent an accurate estimate of the sectionally averaged current through the bay mouth if the subtidal sea level fluctuations in the interior of the bay merely follow those at the coast with no alteration or phase lag.

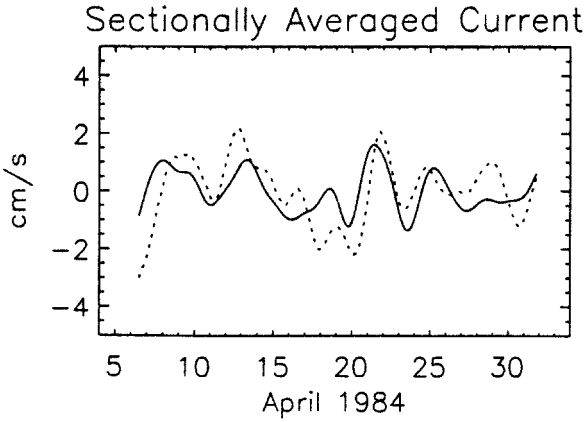

Figure 7. The sectionally averaged current as estimated by the subtidal sea level fluctuations at Cape Henlopen through the continuity requirement ($\langle u_\eta \rangle$, solid line) and the sectionally averaged current computed from current measurements ($\langle u \rangle$, dashed line).

The importance of the remote atmospheric effect on the barotropic response of the estuaries has been demonstrated in a number of systems (Wang and Elliott, 1978; Wang, 1979a; Kjerfve *et al.,* 1978; Schroeder and Wiseman, 1986). A comparison between $\langle u \rangle$ and $\langle u_\eta \rangle$ in Figure 7 shows that the two time series exhibit similar fluctuations. The correlation coefficient between them is about 0.55. It is important to note, however, that there is a sizeable fraction of $\langle u \rangle$ that cannot be explained by $\langle u_\eta \rangle$. This may in part be due to the fact that the coastally forced sea level response may not be spatially uniform within the bay. However, the more significant problem may be that four moorings and seven current meters are less than ideal in resolving all the transverse variability in the structure of the current across the bay mouth.

It can be seen in Figures 6 and 7 that $\langle u \rangle$ is substantially smaller than the observed currents at most mooring locations, especially for the ones over the deep channel. This is caused by the fact that surface and bottom currents over the channel largely cancel each other to yield a small sectionally averaged current. Furthermore, many of the temporal features in the observed currents are not well represented by the sectionally averaged current. It is therefore instructive to examine the effect of local wind forcing over the surface of the bay as a mechanism for producing the observed variability. The solid line in Figure 8 shows the longitudinal component of the wind measured at environmental buoy EB09. The wind is significantly correlated with the near-surface current at mooring 1, suggesting that inflow occurs with the wind blowing upbay. This type of frictional coupling between wind stress and surface current has also been observed in the upper Chesapeake Bay (Wang, 1979b). The near-bottom current in the deep channel is largely against the wind direction, indicating that current at depth may be forced by the wind-induced surface slope. With a wind blowing upbay, the surface slope associated with the local setup would

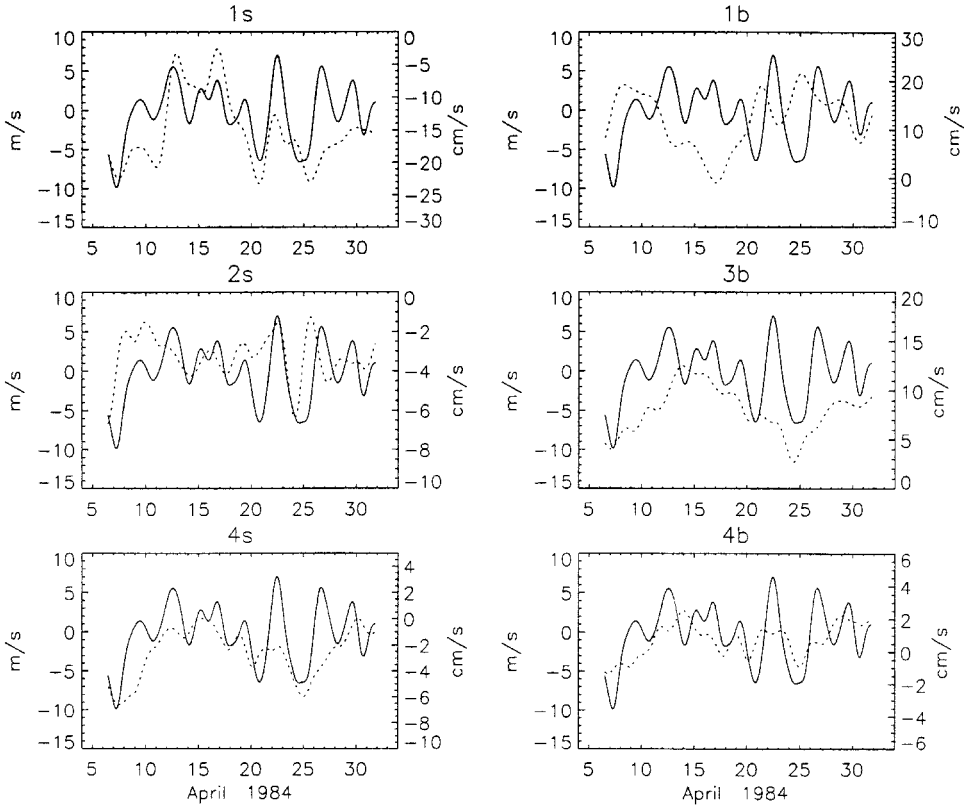

Figure 8. The longitudinal component of wind (solid line) and the subtidal currents (dashed line) at mooring 1s, 1b, 2s, 3b, 4s, and 4b.

drive a return flow near the bottom. In the shallow area off the New Jersey shore (mooring 4) the currents appear to fluctuate with the wind from surface to bottom.

To further examine the role and relative importance of the remote and local effects of atmospheric forcing on the observed currents, empirical orthogonal function (EOF) analysis was conducted on nine time series. These data sets include the longitudinal currents at seven locations across the bay mouth, the longitudinal component of wind (w) at EB09, and the time rate of change of sea level at Cape Henlopen ($d\eta/dt$). Here wind is used to represent the local atmospheric effect and $d\eta/dt$ is used to represent the remote effect (coastal set up). Since the data have mixed units, each of the time series was normalized to unit variance prior to the analysis. Given a total of 9 time series, the EOF method separates any given time series into 9 orthogonal EOF modal series as

$$E_k(t) = \sum_{j=1}^{9} b_j(t) F_{jk}. \tag{1}$$

Table 1. Summary of EOF analysis.

	% Total variance
Mode 1	44.7
Mode 2	18.5
Mode 3	10.9

Here $E_k(t)$ represents the k-th time series, $b_j(t)$ is the j-th EOF modal series and F_{jk} is the normalized multiplication factor (the eigenvector) associated with the j-th modal series for the k-th time series. The EOF method can provide information as to the fraction of the total variance that can be attributed to the j-th mode as well as the fraction of the variance of any time series $E_k(t)$ that can be represented by the j-th mode. The EOF analysis thus gives both an estimate of the overall strength of each mode and an indication of the importance of each mode for each time series.

The results of the EOF analysis show that the first three EOF modes account for 74% of the total variance in all of the time series combined. A breakdown of the fraction of total variance explained by each of the top three modes is shown in Table 1 and the fraction of variance explained by each mode for each time series are shown in Table 2. In addition to a breakdown of the fractional variance explained by each mode, the EOF analysis also provides the eigenvector of each mode for each time series (Table 3). The relative magnitude and sign of the eigenvectors provide information on the spatial structure of the currents for each mode. A positive sign in the eigenvector indicates a positive current flowing into the bay, and vice versa.

The first EOF mode can account for most of the variance for a majority of the current meters. This mode can be interpreted as the response of the system to local wind forcing. Over the deep channel off the Delaware shore a positive wind corresponds to a positive current into the bay. Near the bottom of the deep channel a negative outflow is associated with a positive wind, suggesting that the upwind current there is forced by the wind-induced local setup. In the shallow areas off the New Jersey shore both the surface and bottom currents tend to flow in the wind direction. This transverse structure in the local

Table 2. Percent variance explained by each mode for each time series.

	Mode 1 %	Mode 2 %	Mode 3 %
u (1s)	64.20	2.74	2.70
u (1b)	70.53	10.55	1.34
u (2s)	1.41	54.17	14.18
u (2b)	42.32	14.12	24.14
u (3b)	70.37	5.99	2.75
u (4s)	70.55	10.34	5.39
u (4b)	31.06	25.79	26.60
w	45.00	4.39	0.39
$d\eta/dt$	6.81	38.47	20.57

Table 3. Eigenvectors of each mode for each time series.

	Mode 1	Mode 2	Mode 3
u (1s)	0.40	−0.13	0.17
u (1b)	−0.42	0.25	−0.12
u (2s)	−0.06	0.57	0.38
u (2b)	−0.32	0.29	−0.50
u (3b)	0.42	0.19	0.17
u (4s)	0.42	0.25	−0.23
u (4b)	0.28	0.39	−0.52
w	0.33	0.16	−0.06
$d\eta/dt$	−0.13	0.48	0.46

wind-induced current can be visualized by considering the response of an idealized estuary to a steady local wind along the major axis. The simplest vertically integrated longitudinal momentum balance can be expressed as

$$0 = gH\frac{\partial \eta}{\partial x} + \frac{1}{\rho_0}(\tau_b - \tau_s). \tag{2}$$

Here $\tau_b = -\rho_0 A_z \, (\partial u/\partial z)|_{z=H}$ is the bed stress, τ_s is surface wind stress and H is the water depth at any given point in the estuary's cross-section. With a constant wind stress τ_s, the surface slope is expected to be

$$\frac{\partial \eta}{\partial x} = \frac{\tau_s}{\rho_0 g H_0} \tag{3}$$

where H_0 is the mean depth. The assumption here is that $\partial\eta/\partial x$ does not change across the estuary and the cross-sectionally averaged bottom stress is much smaller than the wind stress or the surface slope (Csanady, 1973). Eqs. (2) and (3) can be combined to yield

$$\tau_b = \tau_s\left(1 - \frac{H}{H_0}\right). \tag{4}$$

In a typical coastal plain estuary with a deep channel and shallow shoals along the shore, Eq. (4) suggests that the bed stress, and hence the current, may carry a significant transverse structure. In the shallow waters along a cross-section where $H < H_0$, τ_b has the same sign as τ_s. In the deeper part of the cross-section where $H > H_0$, the sign of τ_b is opposite to that of τ_s. Since the sign, and therefore direction, of τ_b gives the sign (and direction) of the current just above the bottom, it follows that the near-bottom current changes sign (direction) at the point along the cross-section where the local depth equals the mean depth across the estuary.

In the shallow regions along the shore the effect of surface wind stress dominates over the surface slope to the point where even the near-bottom currents are flowing in the direction of the wind. The currents there are thus directed downwind from surface to

bottom. Over the deep channel the surface current is still in the downwind direction, but the bed stress, and the near-bottom current are now in the upwind direction, as the effect of surface slope dominates that of wind stress at depth. The vertical profile of the longitudinal current over the deep channel thus shows a reversal with depth, with the current in the upper layer flowing with the wind and the current in the lower layer flowing against the wind. This type of transverse structure in the response of estuaries to local wind forcing is consistent with the modeling studies conducted by Csanady (1973) and Signell *et al.* (1990). The second EOF mode is apparently associated with the remote atmospheric effect, with a rise in coastal sea level ($d\eta/dt > 0$) corresponding to positive currents into the bay.

There are significant subtidal fluctuations in salinity at all the mooring locations. These fluctuations can be caused by changes in the river discharge or the wind-induced variability in currents. An inspection of the Delaware River discharge during the study period (Fig. 6) shows that the temporal variation is dominated by only two events. The first event occupies the first half of April. The discharge peaked at a value of 3400 m^3/s on April 7 and then slowly declined to about 600 m^3/s on April 15. The discharge then increased to about 1200 m^3/s on April 18 before it started another slow decline until the end of April. The absence of frequent discharge events suggests that the subtidal salinity fluctuations at several-day time scales are not primarily driven by the variations in the discharge. Instead, the discharge condition may be more important at longer time scales. All the subtidal salinity time series show a trend of decreasing salinity from the beginning to the end of the survey. This long-term trend is especially evident at moorings 2s, 3b, 4s, and 4b where the data indicate a decrease in salinity by about 2 psu over the study period. This long-term trend of decreasing salinity may be due to the response of the bay to the cumulative effect of high river discharge in April.

The subtidal fluctuations in current and salinity are correlated with each other in the deep channel off Cape Henlopen. Generally speaking, a wind-induced inflow would bring high salinity water into the bay, and an outflow would draw water with lower salinity from farther upstream toward the bay mouth. Salinity and current become less coherent in the shallow areas to the right of the channel. It is not clear why the correlation between current and salinity should be lower in this part of the bay mouth. The highly coherent fluctuations in salinity suggest that the same driving mechanism is forcing the salinity fluctuations in this shallow area, and wind-induced variability should be the most likely candidate for producing the observed temporal variations.

It should be noted that the moorings in the shallow waters to the right of the channel show stronger subtidal salinity fluctuations than those found over the deep channel. The standard deviation of salinity at mooring 4s, for example, is 0.83 psu while that at mooring 1s is only 0.55 psu. This is just opposite to the distribution of the magnitude of the subtidal currents. The standard deviation of current at mooring 1s is 5.5 cm/s while that at mooring 4s is only 1.9 cm/s. It appears that the weaker current fluctuations at 4s produce larger salinity fluctuations than the much stronger currents over the channel. This clearly

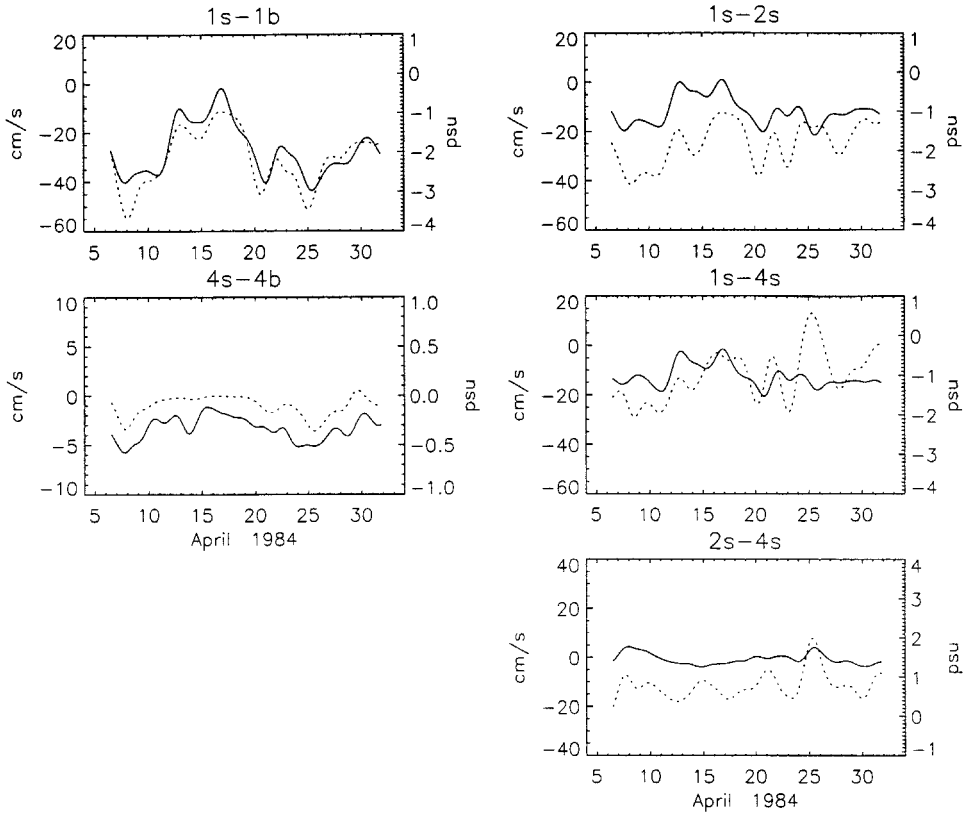

Figure 9. The differences in subtidal currents (solid line) and salinity (dashed line) between the surface and bottom at mooring 1 (1s–1b) and mooring 4 (4s–4b) as well as those between the surface moorings (1s–2s, 1s–4s, and 2s–4s).

indicates that there has to be significant transverse variation in the longitudinal salinity gradient for the observed variability to occur.

Figure 9 shows the surface to bottom differences in current (solid line) and salinity (dashed line) at moorings 1 and 4 as well as the differences between the surface moorings. There are substantial fluctuations in the vertical shear at mooring 1, as the effect of local wind produces subtidal currents in opposite directions. The standard deviation of the vertical shear is 10.7 cm/s. Given a mean current difference of −27.2 cm/s (1s–1b), wind events can substantially modify the overall low frequency current shear. With a wind blowing down the bay, the wind-induced shear would reinforce the mean shear induced by the gravitational circulation, resulting in a marked increase in the overall shear. The setup-induced current brings high salinity water into the bay in the lower layer of the channel and the wind-induced current draws low salinity water out of the bay in the upper layer of the channel. This has the tendency of strengthening the two-layer salinity structure associated with the gravitational circulation and resulted in an enhanced surface to bottom

salinity difference. The reverse situation occurs with an upbay wind. The high correlation (0.91) between the vertical shear and salinity difference at mooring 1 indicates that wind events are extremely important to the vertical salinity structure over the channel.

In the shallow area off Cape May the water is relatively homogeneous and the differences between the surface and bottom currents are small. However, an increase in the vertical shear still corresponds to an enhanced vertical salinity difference at mooring 4. Even though the currents at the surface and bottom are both flowing in the downwind direction, the surface currents are slightly stronger than those at the bottom, resulting in the presence of vertical shear and salinity difference.

In contrast to the high correlation between the vertical shear and vertical salinity difference, the correlation between the transverse shear and transverse salinity difference is poor (Fig. 9). This once again suggests the variation of the time-dependent longitudinal salinity gradient with position across the estuary. Given such circumstance, the transverse shear may be a very poor indicator of the transverse salinity difference at subtidal frequencies.

Figure 9 reveals that the presence of two separate branches of low-salinity water along the shores is a very robust feature. Despite all the subtidal fluctuations, the salinity in the upper layer of the channel (1s) is always lower than that in the central part of the bay (2s). Furthermore, salinity at 2s is always higher than that near the New Jersey shore (4s). This indicates that two branches of low salinity water along the shores are always separated by high salinity water in the central portion of the bay. This type of branched salinity structure has been observed in other estuaries (e.g. Murray and Siripong, 1978). However, the wind-induced variability can produce substantial changes in the vertical and transverse salinity gradients at the bay mouth such that the subtidal salinity distribution on any given day may be quite different from the mean distribution shown in Figure 4. For example, even though the salinity of surface water along the Delaware shore is usually lower than that along the New Jersey shore, wind events on occasion can reverse this situation. Such an event occurred around April 25 when a northerly wind produced an outflow which significantly decreased the salinity near the New Jersey shore. This event also produced a decrease in salinity off the Delaware shore, but the response was much weaker there. As a result, the freshest water on that day resides in the shallow area off Cape May (Fig. 10). The transverse salinity gradient between the surface water over the channel and that in the central portion of the bay is weakened relative to the mean condition, but the transverse salinity gradient between the central part of the bay and the area right off the New Jersey shore is strengthened relative to the mean condition. Over the deep channel, the vertical salinity gradient is strengthened relative to the mean condition as the subtidal current driven by the northerly (downbay) wind reinforces the gravitational circulation in enhancing the two-layer circulation and the vertical salinity gradient there.

5. The tidal variability

Figure 11 shows the high-frequency tidal variations in current and salinity at all the mooring locations. As a common practice, a least-squares harmonic analysis (Dronkers,

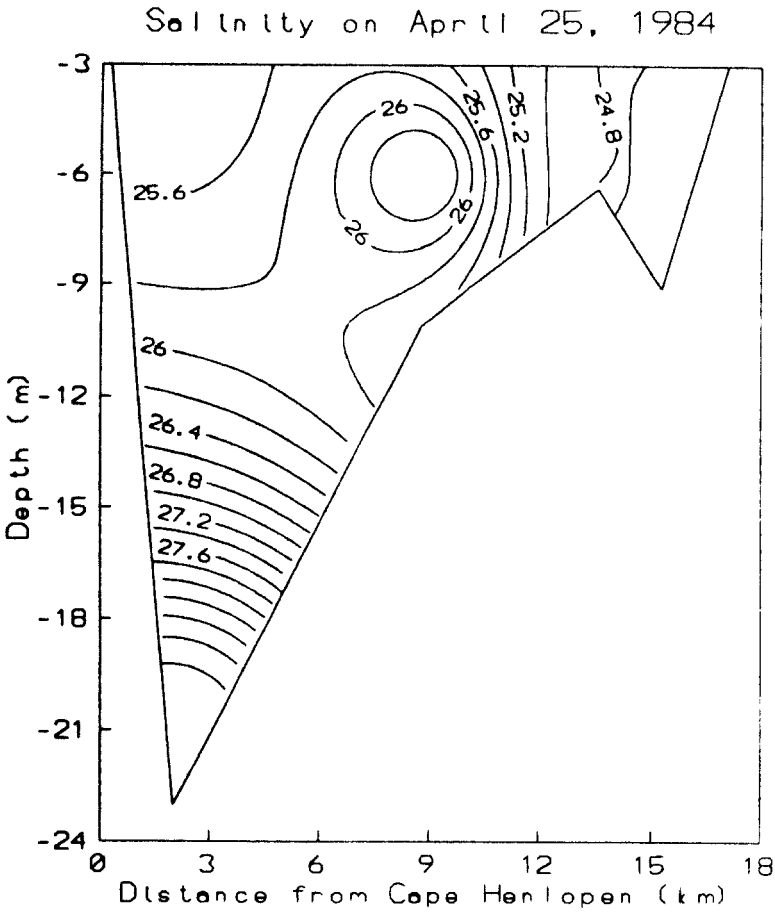

Figure 10. The distribution of salinity across the bay mouth on April 25, 1984. The values are extracted from the subtidal salinity time series at the mooring locations.

1964) is conducted on all the tidal time series. Twelve tidal constituents are included in the analysis, including five diurnal and semidiurnal principal constituents (M_2, N_2, S_2, K_1, and O_1) and other compound and overtides. The results indicate that M_2 is the dominant constituent for the tidal variations in current and salinity. Table 4 summarizes the amplitude and phase of the M_2 variability for both the current and salinity at all the mooring sites. The phase is in degrees relative to the central point of the time series, with a negative phase indicating a phase lag. At each mooring location, predicted time series of salinity and currents are computed based on the 12 harmonic constants. A residual time series is then computed as the difference between the observed and the predicted tidal time series. Table 4 lists the ratio (ϵ) between the variance of the residual time series and that of the observed time series as an indicator for the skill of the harmonic predictions.

Table 4 shows that there is a substantial reduction in the amplitude of the M_2 current with depth. Over the channel at mooring 1, for example, the amplitude of the near bottom

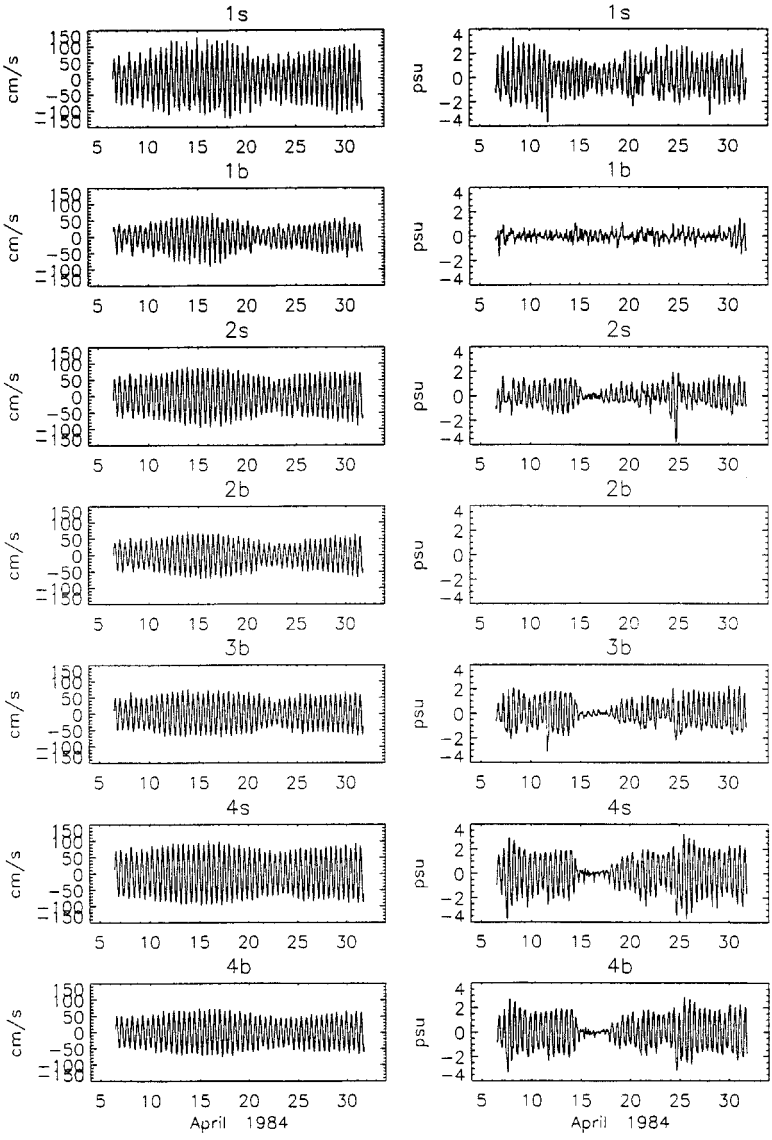

Figure 11. The longitudinal component of tidal currents and the tidal variability in salinity at moorings 1s, 1b, 2s, 2b, 3b, 4s, and 4b.

current (1b) is only about 55% of that near the surface (1s). Furthermore, the near-bottom current there leads that at the surface by about 16°. This phase difference suggests that the tidal currents near the surface and bottom may flow in opposite directions near the time of slack water. Both the decrease in amplitude and increase in phase lead with depth are consistent with the effect of friction on tidal motion. In the shallow waters off the side of

Table 4. Summary of the M_2 tidal characteristics.

	M_2 Current			M_2 Salinity		
	Amplitude (cm/s)	Phase (degrees)	ϵ (%)	Amplitude (psu)	Phase (degrees)	ϵ (%)
1s	82.6	52.6	4.7	0.84	−28.2	68.7
1b	45.7	68.9	7.8	0.32	−26.6	80.3
2s	67.5	53.1	2.0	0.92	−36.0	57.2
2b	48.9	53.5	2.3			
3b	56.7	68.1	2.8	1.21	−22.2	53.8
4s	69.5	67.3	2.5	1.74	−19.0	47.4
4b	56.5	68.8	2.0	1.56	−18.8	48.6

the channel (mooring 2) and near the New Jersey shore (mooring 4), there is also a substantial decrease in the amplitude of the M_2 current with depth. However, there is only a very slight phase difference between the bottom and surface currents. It is not clear why the M_2 currents are nearly in phase from surface to bottom. Perhaps that is due to the fact that the surface and bottom current meters are only 3 m apart. Despite the significant variation in bathymetry across the bay mouth, there is only a modest transverse variation in the amplitude (20%) and phase (15°) of the surface M_2 currents between Cape Henlopen and Cape May.

The harmonic analysis shows that the M_2 variation in salinity is generally in quadrature phase with the M_2 current. This suggests that the M_2 salinity variation is primarily caused by tidal advection. An ebb (negative) current would draw more brackish water from farther upstream of the estuary toward the bay mouth, resulting in a decrease in salinity there. The minimum salinity value is not reached at the time of maximum ebb but at the time of slack water after ebb, resulting in the quadrature phase difference between the current and salinity. Table 4 shows that the largest amplitude of the M_2 salinity variation is found near the New Jersey shore (mooring 4). This is in contrast to the fact that the largest amplitude of the M_2 currents are found over the deep channel. This once again suggests that there are large transverse variations in the longitudinal salinity gradient across the bay mouth.

Table 4 reveals that the tidal currents at all seven locations can be adequately predicted based on the harmonic constants from the 12 tidal constituents. The ratio (ϵ) between the variance of the residual time series and the observed tidal time series is less than 5% for most of the moorings. However, the same cannot be said about the M_2 salinity variability. The ratio (ϵ) between the variance of the residual time series and the observed time series exceeds 50% for a majority of the moorings. The situation is especially serious for the moorings over the deep channel where ϵ reaches 80%. This shows that the predictions made based on the 12 harmonic constants do not adequately represent the observed tidal variability in salinity.

One of the major assumptions of the harmonic analysis is that the amplitude and phase of each constituent remain constant throughout the duration of the time series. This assump-

tion is valid for the tidal currents. It can be seen in Figure 11 that the tidal currents show highly predictable patterns over time. The fortnightly to monthly modulations in the magnitude of the currents are caused by the linear superposition of the M_2 with the weaker N_2 and S_2 tidal currents. These currents are essentially not affected by motions at low frequencies, as the subtidal current fluctuations and mean flow are merely superposed on the tidal currents and can be removed by simply passing the original time series through a low pass filter. However, the effect of the nonlinear interaction between tidal and subtidal motions on the intratidal salinity variability cannot be so removed. For example, a downbay wind has the tendency to bring low salinity water toward the bay mouth at the surface. In that process the longitudinal salinity gradient may be enhanced because low salinity water is brought in closer contact with the more saline shelf water located off the bay mouth. The tidal currents, acting on this enhanced longitudinal salinity gradient, would result in a higher intratidal salinity variability. Two such events can be observed around April 8 and 25 (see Figs. 6 and 8). The event around April 8 corresponds to one day after neap tide while the second event occurs two days after neap tide. For both events the below average tidal excursion should result in a decrease in the intratidal salinity variability, but the opposite is observed (Fig. 11). As a matter of fact, reduced intratidal salinity variations are observed on April 6 and April 23–24 prior to the wind events. The fact that wind events may alter the longitudinal salinity gradients over the subtidal time scales suggests that the magnitude of the intratidal salinity variability may also change over such time scales. This may be one of the reasons why the harmonic analysis based on fixed coefficients cannot adequately represent the observed tidal variability.

In addition to the wind-induced variability, Figure 11 reveals that the intratidal salinity variations are affected by other processes at subtidal time scales. One of the most striking features in Figure 11 is the drastic decrease in the intratidal salinity variations over a three-day period centered around April 16. The intratidal salinity variability is virtually eliminated at moorings 2s, 3b, 4s, and 4b, and the intratidal salinity variability is markedly reduced at mooring 1s. The only mooring that does not show this particular feature is the one located at the bottom of the channel (mooring 1b). Instrument malfunction is not a likely cause of this anomalous feature, as similar features are observed at five out of six moorings. Spring tide occurs on April 15 so one would expect the above average tidal excursion to result in enhanced intratidal salinity variability, but the opposite is observed. Wind events do not appear to play a significant role here, as the subtidal salinity time series shows only a gradual decline in salinity over this three-day period (Fig. 6).

The drastic reduction in the intratidal salinity variability suggests the absence of any significant longitudinal salinity gradient within one tidal excursion of the mooring line. The strong tidal current associated with the spring tide is known to enhance vertical mixing and reduce the degree of stratification. This effect can be represented by a reduction in the modified estuarine Richardson number (Fischer *et al.,* 1979) $R' = (\Delta\rho/\rho)\ (gQ_f/WU^{*3})$. Here $\Delta\rho$ is the vertical density difference, Q_f is river discharge, W is the width of the estuary, and U^* is the shear velocity. Based on a compilation of the experimental data of

Ippen and Harleman (1961) and Rigter (1973), Fischer *et al.* (1979) showed that a decrease in R' corresponds to a decrease in the longitudinal dispersion coefficient K_x and the salt intrusion length L_i. Using an analytical model, McCarthy (1993) has examined the effect of K_x on L_i as well as the longitudinal salinity distribution in estuaries. McCarthy showed that typically the longitudinal salinity distribution can be divided into a central regime in the interior of the estuary where the salinity gradient reaches a maximum and the regimes near the terminal (river and ocean) ends where the salinity gradient is small. He found that both the distribution of the three salinity regimes along the estuary as well as the magnitude of the longitudinal salinity gradient within each regime are very sensitive to the magnitude of K_x. The observed anomalous feature may reflect the fact that the enhanced vertical mixing associated with a strong spring tide could significantly affect the characteristics of longitudinal salt dispersion which in turn changes the longitudinal gradient near the mooring sites.

The second spring tide occurs on April 30. The tidal currents associated with this event are only slightly weaker than those from the first spring tide, but all the moorings show increased intratidal salinity variations. It is not clear why the intratidal salinity variations during the first spring tide are so different from those in the second spring tide. Perhaps a critical R' has to be reached before it can have a significant impact on the longitudinal salinity gradient around the mooring sites. However, this type of discrepancy no doubt contributes to the poor skill of the harmonic analysis. Additional studies are required to resolve this issue.

Figure 12 shows the surface to bottom differences in current and salinity at moorings 1 and 4 as well as the differences between the surface moorings. The surface to bottom salinity difference (ΔS) at mooring 1 over the deep channel shows large intratidal variations of up to ± 2 psu. There are significant long term variations in the magnitude of ΔS which cannot be easily explained by the spring-neap tidal modulations. Stratification is supposed to be enhanced during neap tides, but no significant increases in ΔS are observed on either the first (April 7) or the second (April 22) neap tide. Stratification does decrease after the first spring tide (April 16), but the magnitude of ΔS remains large during the second spring tide (April 30). Part of the reason for such complicated behavior may be due to the fact that the magnitude of ΔS is controlled by a combination of spring-neap modulation and the wind-induced subtidal variability. Take the ΔS at mooring 4 for example, the largest magnitudes of ΔS are observed one day after the first neap tide (April 8) and three days after the second neap tide (April 25). Both events correspond to a downbay wind which draws low salinity water toward the bay mouth and enhances the longitudinal salinity gradient. The increased longitudinal salinity gradient may then enhance the tidal straining effect in producing a larger intratidal variation in ΔS.

There are large intratidal variations in the transverse salinity gradient. The difference between mooring 1s off Cape Henlopen and mooring 4s off Cape May can reach ± 4 psu. This is much greater than the mean difference of 0.9 psu between the two sites. Given the large intratidal variability in the transverse salinity gradient, the salinity structure across

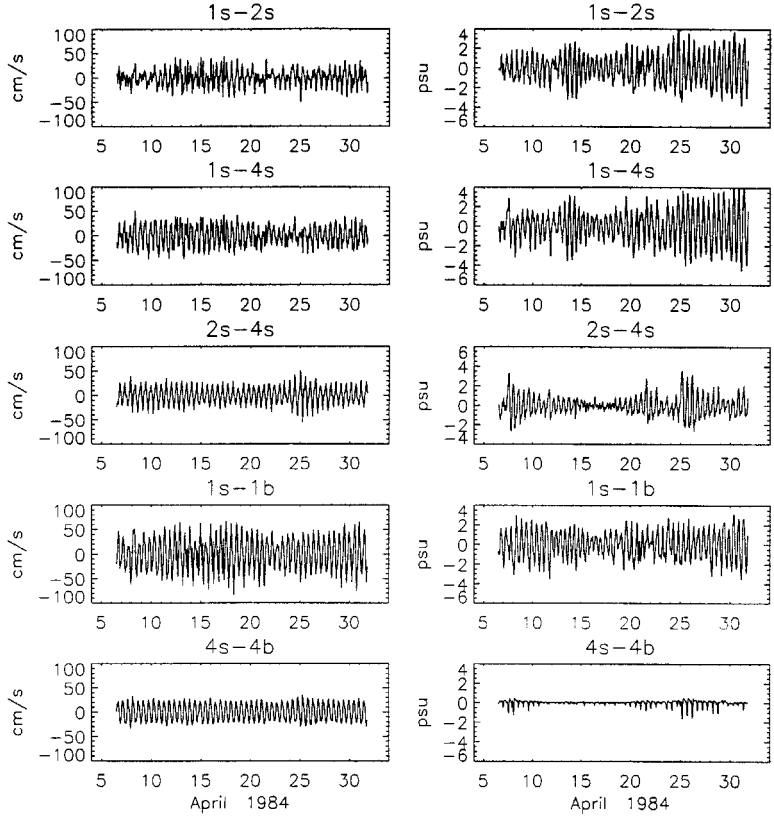

Figure 12. The differences in the tidal currents and salinity between the surface and bottom at mooring 1 (1s–1b) and mooring 4 (4s–4b) as well as those between the surface moorings (1s–2s, 1s–4s, and 2s–4s).

the bay mouth at any given phase of the tidal cycle may totally obscure the mean salinity distribution shown in Figure 4. This indicates that any sampling scheme across the bay mouth must have a sufficiently high sampling rate to prevent the potentially serious problem of tidal aliasing from occurring.

Figure 13 shows plots of tidal velocity shear versus salinity difference between the surface and bottom at moorings 1 and 4 as well as those between the surface moorings. In general, the correlation is very poor between the vertical tidal shear (ΔU) and surface to bottom salinity difference (ΔS). This is in sharp contrast to the high correlation between ΔU and ΔS at subtidal frequencies. Furthermore, the horizontal velocity shear and salinity difference between 1s and 4s are virtually uncorrelated, indicating that the transverse shear is also a very poor indicator of the transverse salinity difference.

Of the three time scales examined (the mean, subtidal, and tidal), the high frequency tidal currents are the most predictable, as they are forced by deterministic mechanisms. However, the opposite may be true when salinity is concerned, as the intratidal variability in salinity may be the most difficult to understand. The intratidal salinity variability at any

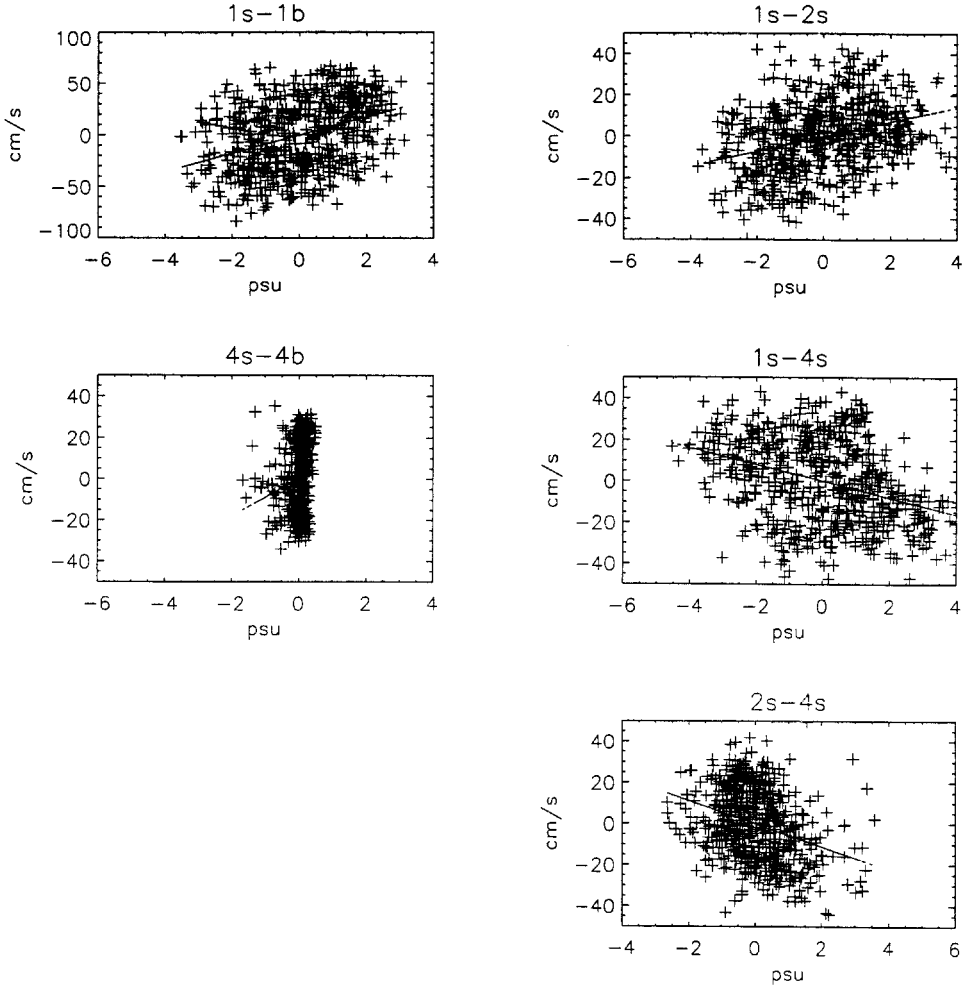

Figure 13. Plots of current difference versus salinity difference between the surface and bottom at mooring 1 (1s–1b) and mooring 4 (4s–4b) as well as those between the surface moorings (1s–2s, 1s–4s, and 2s–4s).

fixed position is controlled by a combination of tidal advection, mixing and straining. Furthermore, the characteristics of the intratidal salinity variability may change significantly over the subtidal time scales due to the nonlinear interactions between the tidal and subtidal motions as well as the effect of spring-neap modulation. All of these make the prediction of tidal variations in salinity very difficult.

6. The residual salt flux

The tidally averaged residual salt flux through the bay mouth can be expressed as

$$Q = \frac{1}{T}\int_0^T \left\{ \int_0^b \int_0^h [u(y, z, t)\, s(y, z, t)]\, dy\, dz \right\} dt. \tag{5}$$

Here Q is the residual salt flux, T is the tidal period, b is the breadth of the estuary, h is the depth, $u(y, z, t)$ is the longitudinal current and $s(y, z, t)$ is salinity. Eq. (5) can be written in a more concise form as

$$Q = \overline{\langle u(y, z, t)\, s(y, z, t)\rangle} \tag{6}$$

where the angle brackets indicate cross-sectional integral and the overbar denotes a temporal average over the tidal cycle. Normally Q represents a single value representing the mean flux over one tidal cycle.

In the present study concurrent measurements of current and salinity are available from six positions across the bay mouth. An attempt is made to estimate Q based on these measurements. The determination of a single tidal period T may cause some problem, as more than one tidal constituents are at work here. However, with long-term time series data this problem can be easily sidestepped. Instead of calculating a residual flux based on one fixed period, the instantaneous sectionally integrated flux can be low-pass filtered to yield the subtidal fluctuations in the residual salt flux $Q(t)$. In short, the overbar in Eq. (6) now represents a low-pass filter operation.

At each position across the bay mouth transect (y, z), the temporal variations in the current and salinity can be decomposed as

$$\begin{aligned} u(t) &= u_0 + u_s(t) + u_T(t) \\ s(t) &= s_0 + s_s(t) + s_T(t). \end{aligned} \tag{7}$$

Here the subscript "0" denotes mean value averaged over the entire study period, "s" denotes subtidal fluctuations and "T" represents tidal variability. The decomposition shown in Eq. (7) can be accomplished by passing the individual time series through a low-pass filter. With Eqs. (6) and (7), the residual salt flux can be represented as

$$\begin{aligned} Q(t) &= \overline{\langle us\rangle} \\ &= [\langle u_0 s_0\rangle + \overline{\langle u_0 s_s\rangle} + \overline{\langle u_0 s_T\rangle}] \\ &\quad + [\overline{\langle u_s s_0\rangle} + \overline{\langle u_s s_s\rangle} + \overline{\langle u_s s_T\rangle}] \\ &\quad + [\overline{\langle u_T s_0\rangle} + \overline{\langle u_T s_s\rangle} + \overline{\langle u_T s_T\rangle}]. \\ &= [A] + [B] + [C]. \end{aligned} \tag{8}$$

The three terms in $[A]$ represent the effect of salt advection by the mean flow. The dominant term here is $\langle u_0 s_0\rangle$ which includes the salt flux due to the river outflow and the density-induced gravitation circulation. The remaining two terms are negligible.

The three terms in $[B]$ represent the advection of salt by the wind-induced subtidal current fluctuations. $\overline{\langle u_s s_0\rangle}$ represent the salt flux due to the advection of the mean salinity distribution by the subtidal currents. $\overline{\langle u_s s_s\rangle}$ represents the residual salt flux due to the temporal and spatial correlations in the subtidal current and salinity fluctuations. $\overline{\langle u_s s_T\rangle}$ comes from the spatial and temporal correlations between the subtidal currents and the

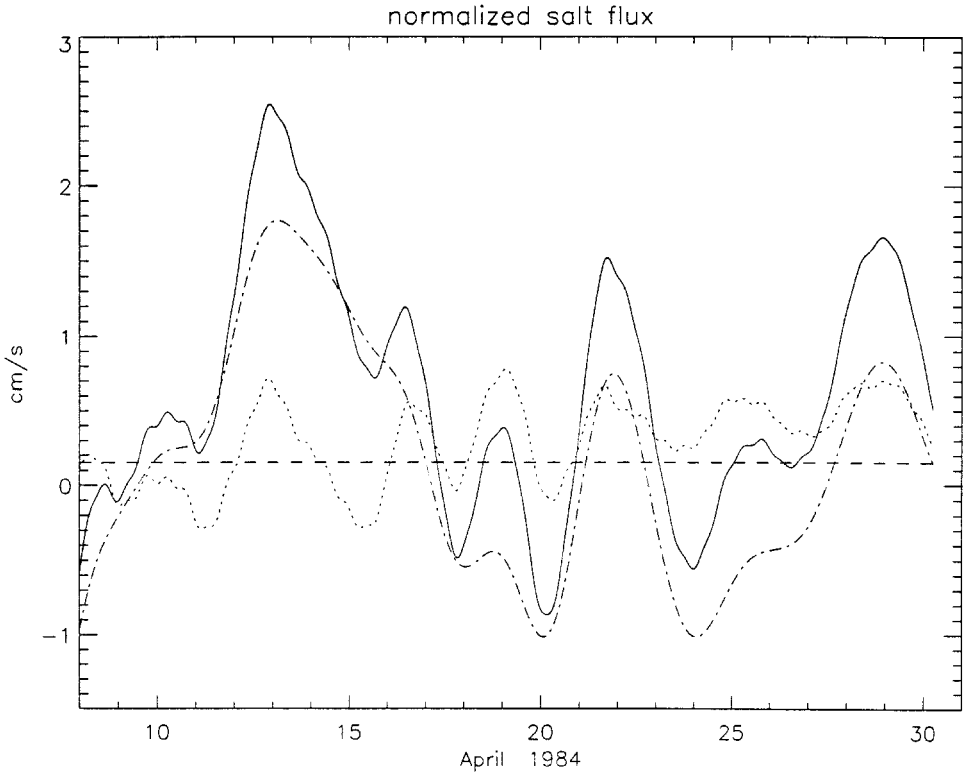

Figure 14. The subtidal fluctuations in the total normalized salt flux through the bay mouth (solid line). Also plotted are the contributions from the advection of salt by the wind-induced subtidal currents (dash-dotted line), the tidal pumping effect (dotted line), and the mean flow (dashed line).

tidal variability in salinity. Calculations of the three terms based on observed data indicate that $\overline{\langle u_s s_0 \rangle}$ is the leading term here, followed by a much smaller $\overline{\langle u_s s_s \rangle}$. The term $\overline{\langle u_s s_T \rangle}$ is negligible.

The three terms in $[C]$ represent the residual salt flux from the advection of salt by the tidal currents. The dominant term here is $\overline{\langle u_T s_T \rangle}$, which comes from the spatial and temporal correlations in the tidal variations in salinity and current. This term can be interpreted as the contribution from the tidal pumping effect (Geyer and Nepf, 1996; Hunkins, 1981).

The solid line in Figure 14 shows the total residual salt flux Q as computed from $\overline{\langle us \rangle}$. The salt flux per unit area has been normalized by the sectionally and temporally averaged salinity across the bay mouth ($\langle s_0 \rangle = 27.52$ psu) to yield a unit of cm/s. Figure 14 also shows the three leading terms which contribute to the total residual salt flux. In terms of their relative importance, these terms are $\overline{\langle u_s s_0 \rangle}$ (dash-dotted line), $\overline{\langle u_T s_T \rangle}$ (dotted line), and $\langle u_0 s_0 \rangle$ (dashed line). There are significant subtidal fluctuations in the residual salt flux. It's not surprising that the leading factor for producing these subtidal fluctuations represents the advection of salt by the wind-induced subtidal currents. It should be noted that the tidal

pumping effect is the second most important term. This suggests that the co-variations in the structure of salinity and current at tidal frequencies may be very important to the overall residual salt transport in a coastal plain estuary such as the Delaware Bay.

7. Concluding remarks

The results of this study show that the presence of significant transverse variability is an integral part of the response of a coastal plain estuary to a variety of forcing mechanisms over a wide spectrum of frequencies. These mechanisms include the river-induced baroclinic motion which determines the long-term distributions, the wind-induced variability which operates at several-day periods, and the tidally-induced variability at diurnal and semidiurnal periods.

The long-term distribution associated with the river-induced gravitational circulation is characterized by the presence of two branches of buoyant outflow in the shallow areas along the shores separated by a more saline inflow concentrating in the deep channel and the central portion of the bay. The long-term residual longitudinal pressure gradient consists of a down-bay directed surface slope and an up-bay directed baroclinic pressure gradient. Since the baroclinic pressure gradient is proportional to the vertically integrated longitudinal density gradient, it is overwhelmed by the surface slope over the shoals, resulting in two branches of buoyant outflow along the shores.

At subtidal frequencies, the fluctuations in current and salinity are largely controlled by the effect of local wind. Over the deep channel, the effect of local wind produces down-wind current in the upper layer and up-wind current in the lower layer. In deeper water, wind stress does not overwhelm the pressure gradient throughout the water column and a return flow develops at depth. Over the shallow shoals wind stress dominates over the pressure gradient and produces down-wind current throughout the water column. A wind blowing down the estuary thus has the tendency of reinforcing the gravitational circulation in enhancing the vertical shear and vertical salinity difference over the channel. A wind blowing up the estuary has the opposite effect.

At the semidiurnal and diurnal tidal frequencies the current and salinity exhibit substantial transverse variations of ± 50 cm/s and ± 4 psu, respectively. These variations can easily overwhelm the transverse structure associated with the river and wind-induced variability. Tidal aliasing is therefore a serious problem for any sampling scheme which does not resolve the intratidal variability in the transverse structure.

The instantaneous transverse structures of current and salinity are forced by all the above-mentioned mechanisms over very different time scales. To first order these mechanisms interact linearly by simply superimposing on top of one another. If these interactions were strictly linear then the effect of each mechanism on the current and salinity can be separated based on the frequencies involved. However, there is evidence that mechanisms at different frequencies may interact nonlinearly to produce the observed variability. This is particularly evident for the long-term variations in the intratidal salinity variability, as features that deviate from a deterministic pattern can be more easily identified. The results

show that wind-induced variability may change the intratidal salinity variability over the subtidal time scales through its effect on the ambient longitudinal salinity gradient. There is also evidence that the spring-neap tidal modulation affects not only the vertical salinity gradient but also the longitudinal salinity gradient over the fortnightly time scale.

A calculation of the residual advective salt flux shows the presence of significant subtidal fluctuations in the salt transport. The advection of salt by the wind-induced subtidal current is the leading factor for producing the observed residual salt flux. However, the effect of tidal pumping also contributes significantly to the overall residual salt flux. Given the fact that the across-estuary variations in current and salinity are of the same order of magnitude as their counterparts in the vertical dimension, it is essential to take the transverse variability into consideration for salt flux calculations.

Additional studies are needed to examine many issues that cannot be adequately addressed here. These include, among other things, the sizable fraction of variance in the subtidal currents that cannot be accounted for by the effects of remote and local atmospheric forcing. The mechanisms which produce the apparent transverse variation in the longitudinal salinity gradient need to be assessed. Furthermore, an in-depth analysis is required to determine the factors which control the intratidal variability in salinity. Studies with enhanced spatial resolution, such as those from ADCP and scanfish surveys, are required to fully resolve the transverse variability in current and salinity in such a coupled estuary-shelf system.

Acknowledgments. This study was funded by the National Science Foundation under grant OCE-9000158. Support was also provided by NOAA Sea Grant under grant NA56RG0147 (project R/ME-16) Randy Zagar provided programing support for some of the graphics. Jacqueline Bijansky typed the manuscript.

REFERENCES

Bloomfield, P. 1976. Fourier Analysis of Time Series: An Introduction, John Wiley & Sons, New York, 258 pp.

Csanady, G. T. 1973. Wind-induced barotropic motion in long lakes. J. Phys. Oceanogr., *3,* 429–438.

Dronkers, J. J. 1964. Tidal Computations in Rivers and Coastal Waters, North-Holland, New York, 518 pp.

Dyer, K. R. 1974. The salt balance in stratified estuaries. Estuar. Coastal Mar. Sci., *2,* 273–281.

Fischer, H. B. 1972. Mass transport mechanism in partially stratified estuaries. J. Fluid Mech., *53,* 671–687.

Fischer, H. B., E. J. List, R. C. Y. Koh, J. Imberger and N. D. Brooks. 1979. Mixing in Inland and Coastal Waters. Academic Press, New York. 483 pp.

Friedrichs, C. T. and J. M. Hamrick. 1996. Effects of channel geometry on cross sectional variations in along channel velocity in partially stratified estuaries, *in* Buoyancy Effects on Coastal and Estuarine Dynamics, D. G. Aubrey and C. T. Friedrichs eds., Coastal and Estuarine Studies, Vol. 23, American Geophysical Union, 285–300.

Garvine, R. W. 1985. A simple model of estuarine subtidal fluctuation forced by local and remote wind stress. J. Geophys. Res., *96*(C6), 11945–11948.

—— 1991. Subtidal frequency estuary-shelf interaction: Observations near Delaware Bay. J. Geophys. Res., *96*(C4), 7049–7064.

Geyer, W. R. and H. Nepf. 1996. Tidal pumping of salt in a moderately stratified estuary, *in* Buoyancy Effects on Coastal and Estuarine Dynamics, D. G. Aubrey and C. T. Friedrichs, eds., Coastal and Estuarine Studies, Vol. 23, American Geophysical Union, 213–226.

Hunkins, K. 1981. Salt dispersion in the Hudson estuary. J. Phys. Oceanogr., *11,* 729–738.

Hunter, J. R. and C. J. Hearn. 1987. Lateral and vertical variations in the wind-driven circulation in long, shallow lakes. J. Geophys. Res., *92,* 13,106–13,114.

Huzzey, L. M. 1988. The lateral density distribution in a partially mixed estuary. Estuar. Coast. Shelf Sci., *9,* 351–358.

Huzzey, L. M. and J. M. Brubaker. 1988. The formation of longitudinal fronts in a coastal plain estuary. J. Geophys. Res., *93*(C2), 1329–1334.

Ippen, A. T. and D. R. F. Harleman. 1961. One Dimensional Analysis of Salinity Intrusion in Estuaries, U.S. Army Corps of Engineers, Waterways Experimental Station, Vicksburg, Mississippi, Technical Bull. No. 5.

Kjerfve, B. 1978. Bathymetry as an indicator of net circulation in well mixed estuaries. Limnol. Oceanogr., *23,* 816–821.

—— 1986. Circulation and salt flux in a well mixed estuary, *in* Physics of Shallow Estuaries and Bays, Coastal Estuarine Studies, *16,* D. A. Wolfe, ed., Academic, San Diego, California, 63–81.

Kjerfve, B., J. E. Greer and R. L. Crout. 1978. Low-frequency response of estuarine sea level to non-local forcing, *in* Estuarine Interactions, M. L. Wiley, ed., Academic Press, San Diego, California, 497–513.

Kjerfve, B. and J. A. Proehl. 1979. Velocity variability in a cross-section of a well-mixed estuary. J. Mar. Res., *37,* 409–418.

Klavens, A., P. Stone and G. Stoney. 1986. Delaware River and Bay circulation survey: 1984–1985, NOS Oceanography Circulation Survey Report, 9, U. S. Dept of Commerce, NOAA, 79 pp.

McCarthy, R. K. 1993. Residual currents in tidally dominated, well-mixed estuaries. Tellus, *45A,* 325–430.

Murray, S. P. and A. Siripong. 1978. Role of lateral gradients and longitudinal dispersion in the salt balance of a shallow, well-mixed estuary, *in* Estuarine Transport Processes, B. Kjerfve, ed., University of South Carolina Press, Columbia, South Carolina, 113–124.

Pritchard, D. W. 1952. Salinity distribution and circulation in the Chesapeake estuarine system. J. Mar. Res., *11,* 106–123.

—— 1956. The dynamic structure of a coastal plain estuary. J. Mar. Res., *15,* 33–42.

Rigter, B. P. 1973. Minimum length of salt intrusion in estuaries. J. Hydraul. Div. Proc. Am. Soc. Div. Eng., *99,* 1475–1496.

Schroeder, W. S. 1978. Riverine influence on estuaries: A case study, *in* Estuarine Interactions, M. L. Wiley, ed., Academic, San Diego, California, 347–364.

Schroeder, W. S. and W. J. Wiseman. 1986. Low-frequency shelf-estuarine exchange processes in Mobile Bay and other estuarine systems on the northern Gulf of Mexico, *in* Estuarine Variability, D. A. Wolfe, ed., Academic Press, New York, 355–367.

Signell, R. P., R. C. Beardsley, H. C. Grabor and A. Capotondi. 1990. Effect of wave-current interaction on wind-driven circulation in narrow, shallow embayments. J. Geophys. Res., *95*(C6), 9671–9678.

Valle-Levinson, A. and K. M. M. Lwiza. 1995. The effects of channels and shoals on exchange between the Chesapeake Bay and the adjacent ocean. J. Geophys. Res., *100*(C9), 18,551–18,563.

—— 1997. Bathymetric influences on the lower Chesapeake Bay hydrography. J. Mar. Syst., *12,* 221–236.

Valle-Levinson, A., K. M. M. Lwiza and B. D. Connally. 1994. Flow lateral structure in the lower Chesapeake Bay. EOS Trans. Amer. Geophys. Union, Supplement, *75*(16), 198.

Valle-Levinson, A. and J. O'Donnell. 1996. Tidal interaction with buoyancy-driven flow in a coastal plain estuary, *in* Buoyancy Effects on Coastal and Estuarine Dynamics, D. G. Aubrey and C. T. Friedrichs, eds., Coastal and Estuarine Studies, Vol. 23, American Geophysical Union, 265–281.

Wang, D.-P. 1979a. Subtidal sea level variation in Chesapeake Bay and relations to atmospheric forcing. J. Phys. Oceanogr., *9,* 413–421.

—— 1979b. Wind-driven circulation in the Chesapeake Bay, Winter 1975. J. Phys. Oceanogr., *9,* 564–572.

Wang, D.-P. and A. J. Elliott. 1978. Nontidal variability in the Chesapeake Bay and Potomac River: Evidence for nonlocal forcing. J. Phys. Oceanogr., *8,* 225–232.

Wong, K.-C. 1994. On the nature of transverse variability in a coastal plain estuary. J. Geophys. Res., *99*(C7), 14,209–14,222.

Wong, K.-C. and R. W. Garvine. 1984. Observations of wind-induced, subtidal variability in the Delaware estuary. J. Geophys. Res., *89*(C6), 10,589–10,597.

Wong, K.-C. and A. Münchow. 1995. Buoyancy forced interaction between estuary and inner shelf: observations. Continental Shelf Res., *15,* 59–88.

Received: *6 May, 1997;* revised: *16 October, 1997.*